Supplementary Information:
Noise suppression via pulsed all-optical magnetometry with nitrogen-vacancy ensembles

Xiechen Zheng,[1,2] Jeyson Támara-Isaza,[2,3] John W. Blanchard,[2] and Ronald L. Walsworth[1,2,4]

[1] *Department of Electrical and Computer Engineering, University of Maryland, College Park, MD 20742, USA*
[2] *Quantum Technology Center, University of Maryland, College Park, MD 20742, USA*
[3] *Departamento de Física, Universidad Nacional de Colombia, sede Bogotá, Carrera 45, Colombia*
[4] *Department of Physics, University of Maryland, College Park, MD 20742, USA*

(Dated: July 1, 2026)

Contents

Supplementary Note 1. AO-PL features from short signal readout timing (t_r)

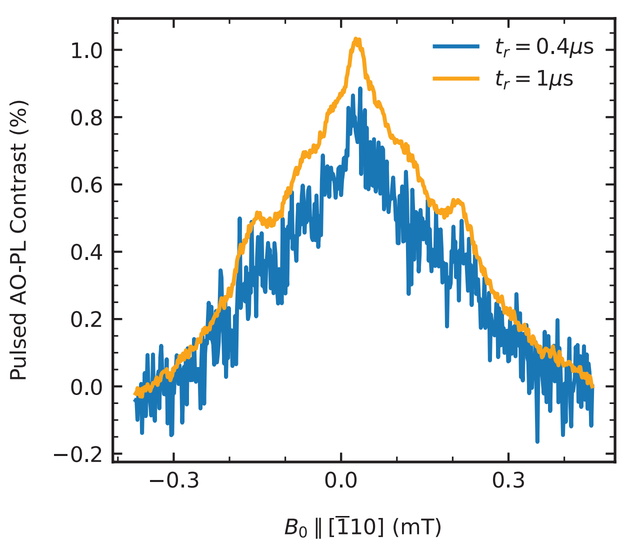

Supplementary Fig. 1. Pulsed AO-PL contrast of sample D1 measured for signal readout pulse values $t_r = 0.4\,\mu$s and $t_r = 1\,\mu$s, with dark time $\tau = 2\,$ms. $t_r < 1\,\mu$s yields weaker AO-PL contrast and worse SNR due to poor optical spin polarization after the optical pulse.

Suppl. Fig. 1 shows a comparison of measured near-zero-field pulsed AO-PL contrast features for sample D1, with fixed dark time $\tau = 2\,$ms, and for signal readout pulse values $t_r = 0.4\,\mu$s and $t_r = 1\,\mu$s. The result with $t_r = 0.4\,\mu$s exhibits weaker AO-PL contrast and worse SNR. The weaker AO-PL contrast is attributed to poor optical spin polarization shortly after the optical pulse, as a longer τ allows the NV electronic spins to relax toward thermal equilibrium. In addition, the lower PL emission intensity lead to worse SNR. For t_r between $0\,\mu$s and $0.4\,\mu$s, the near-zero-field AO-PL contrast features are no longer identifiable in measurement with our setup.

Supplementary Note 2. Differences of polarization lifetime (T_1) measurements between on- and off-resonance magnetic fields

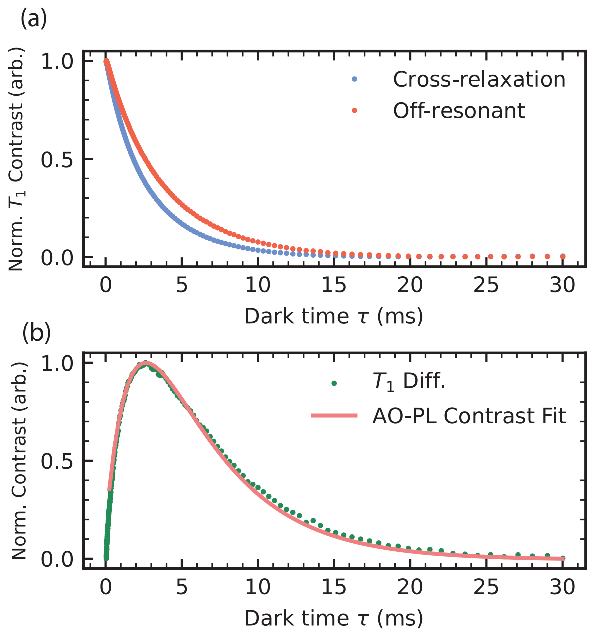

Supplementary Fig. 2. (a) Experimentally-determined NV ground-state spin-polarization lifetime (T_1) of sample D1 as a function of dark time τ. Fits of pulsed AO-PL decay (not shown) yield $T_1 = 2.602 \pm 0.008\,$ms with cross-relaxation magnetic field at $B_0 = 0.03\,$mT, and $T_1 = 3.70 \pm 0.012\,$ms with off-resonant magnetic field at $B_0 = 0.45\,$mT. (b) Differences of T_1 results in Suppl. Fig. 2(a) and a bi-exponential fit to the measured AO-PL contrast of sample D1 in Fig. 3(a) of the main text as a function of dark time τ, with good consistency found between the methods.

Suppl. Fig. 2(a) presents the experimentally-determined NV ground-state spin-polarization lifetime (T_1) of sample D1 as a function of dark time τ from 0 to $30\,\mu$s, using the relaxometry pulse sequence shown in Fig. 1(b) of the main text. The normalized pulsed AO-PL $S(\tau)$ measurements are fit with a stretched exponential function (not shown in Suppl. Fig. 2(a)) with a stretched factor β as:

$$S(\tau) = A(1 + \exp(-(\frac{\tau}{T_1})^{\beta})) \tag{S1}$$

When NV-NV cross-relaxation is strongest at magnetic field $B_0 = 0.03\,$mT, the fit yields $T_1 = 2.602 \pm 0.008\,$ms, with $\beta = 0.926 \pm 0.004$. At the off-resonant magnetic field $B_0 = 0.45\,$mT, $T_1 = 3.7 \pm 0.012\,$ms, with $\beta = 0.976 \pm 0.004$.

Suppl. Fig. 2(b) shows the normalized difference between these two T_1 relaxometry measurements alongside the normalized bi-exponential fit of pulsed AO-PL contrast as a function of τ presented in Fig. 3(a, blue) of the main text. The good agreement between these normalized results indicate that the optimal τ for achieving maximum AO-PL contrast is linked to the differences of T_1 between cross-relaxation and off-resonant conditions, and is therefore dependent on the NV concentration.

Supplementary Note 3. Comparison of near-zero-field AO-PL contrast features between pulsed and cw operations with additional optical intensity noise

Fig. 4(b) in the main text demonstrates the enhanced noise suppression achieved with pulsed AO operation, using a test signal at $f_{\text{test}} = 43\,$Hz with additional amplitude modulation (AM) noise at 0.2% depth and 200 Hz bandwidth applied to the AOM RF power. To further evaluate the noise suppression performance, we increase the AM depth to 1% and compare the measured near-zero-field AO-PL contrast features of sample D1 for cw and pulsed operation,

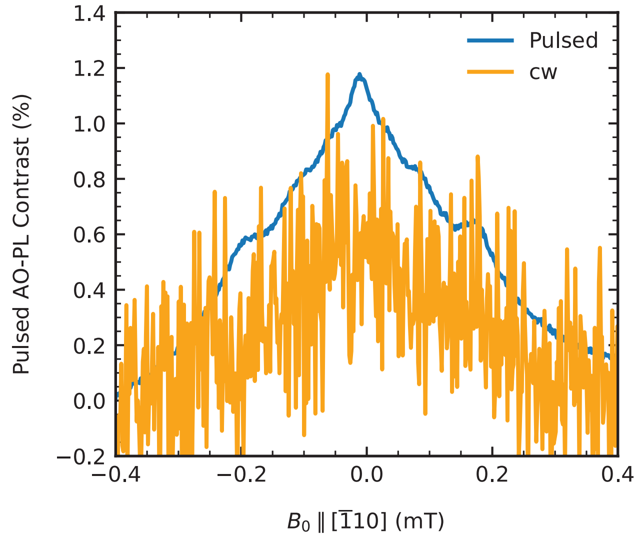

Supplementary Fig. 3. Measured near-zero-field AO-PL contrast of sample D1 using pulsed (blue) and cw (orange) methods as a function of B_0. Additional optical intensity noise is applied through AM with 1% depth and 200 Hz bandwidth from noise modulation of the AOM RF power. The pulsed method can still resolve clear AO-PL contrast features under substantial optical intensity noise.

as shown in Suppl. Fig. 3. The wall time for both measurements is kept approximately identical to ensure a fair comparison, as cw AO measurements have a higher sampling rate and average more data points at each magnetic field. The results show that while the cw technique fails to resolve AO-PL contrast features with good SNR under strong optical noise, the pulsed technique maintains good robustness. This result highlights the advantage of the pulsed method for resolving AO-PL contrast features during applied magnetic field sweeps, which are typically slower than measuring an oscillating (AC) magnetic signal at a fixed bias field.

Supplementary Note 4. Pulsed AO-PL contrast from spin-state mixing

Suppl. Fig. 4 shows experimental results for pulsed AO-PL contrast as a function of $B_1 \parallel [100]$ and $B_2 \parallel [010]$, using sample D3 with approximately 0.3 ppm NV concentration (top) and sample D1 with approximately 3.8 ppm NV concentration (bottom), respectively. We vary both B_1 and B_2 from 0 to 1.5 mT, with step size approximately 0.04 mT. The lower NV concentration in sample D3 allows for the measurement of AO-PL contrast from NV electronic spin states mixing under applied magnetic fields that are not aligned with the NV quantization axis, as the AO-PL contrast arising from NV-NV cross-relaxation is much weaker [1]. We plot the pulsed AO-PL contrast from I_{sig} at $t_r = 1\,\mu$s [Suppl. Fig. 4(a)], I_{ref} at $t_r = 79\,\mu$s [Suppl. Fig. 4(b)], and normalized values using the steps described in Sec. III of the main text [Suppl. Fig. 4(c)]. Each two-dimensional AO-PL contrast plot is normalized to the maximum intensity from a given scan of (B_1, B_2). By implementing two PL readout normalization with sample D3, we successfully measure pulsed AO-PL contrast from spin-state mixing as a non-negligible background, along with contributions from weak NV-NV cross-relaxation as stripelike features [Suppl. Fig. 4(c, top)]. A stronger background spin-state mixing pulsed AO-PL contrast is observed in the reference readout measurement [Suppl. Fig. 4(b, top)] compared to the signal readout measurement [Suppl. Fig. 4(a, top)]. This result differs from that of sample D1, where pulsed AO-PL contrast arising from NV-NV cross-relaxation is primarily observed in the signal readout window [Suppl. Fig. 4(a, bottom)], as described in Sec. III of the main text. These findings suggest that the pulsed AO technique can be adapted to measure AO-PL contrast using various measurement protocols under a wide range of applied magnetic fields. Optimizing AO pulse sequences for specific operational conditions will be explored in future studies.

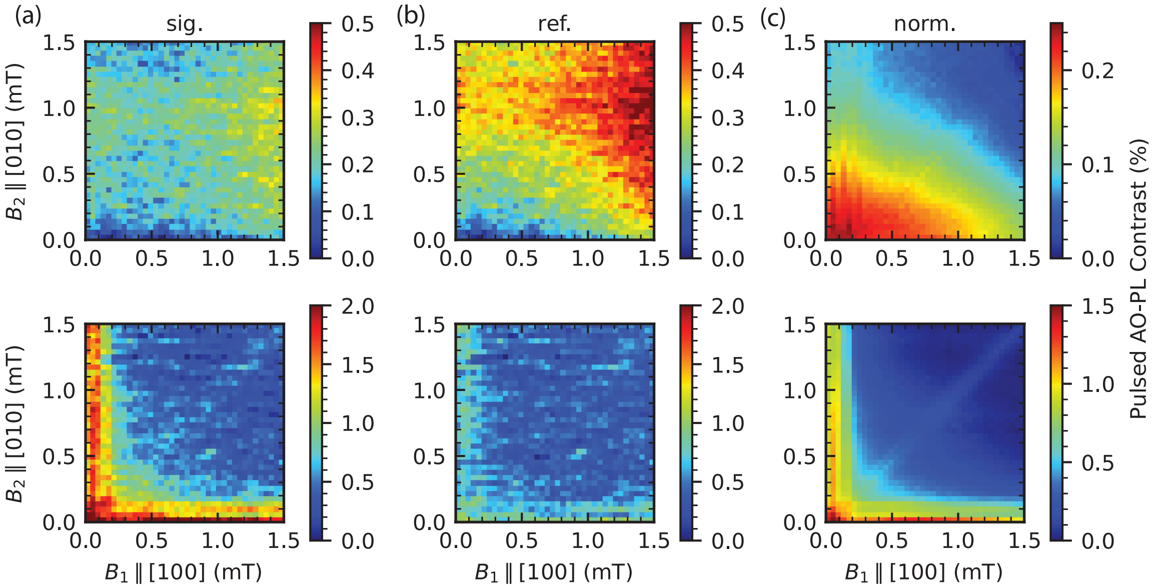

Supplementary Fig. 4. Pulsed AO-PL contrast as a function of applied magnetic field magnitude and direction, for: (a) signal readout pulse value $t_r = 1\,\mu$s; (b) reference readout pulse value $t_r = 79\,\mu$s; and (c) after normalization, using sample D3 with ≈ 0.3 ppm [NV] (top) and sample D1 with ≈ 3.8 ppm [NV] (bottom). Implementing two PL readout normalization with sample D3 allows the characterization of pulsed AO-PL contrast from both spin-state mixing as a non-negligible background and weak NV-NV cross-relaxation as stripelike features. Unlike pulsed AO-PL contrast from NV-NV cross-relaxation, which is primarily observed in the signal readout measurement (a, bottom), a significant portion of pulsed AO-PL contrast from spin-state mixing appears in the reference readout measurement (b, top). Future studies will explore optimizing AO pulse sequences for specific operational conditions.

[1] X. Zheng, J. Támara-Isaza, Z. Yin, J. Cremer, J. W. Blanchard, C. A. Hart, M. Crescimanno, P. V. Petruzzi, M. J. Turner, and R. L. Walsworth, All-optical photoluminescence response of nitrogen-vacancy ensembles in diamond at low magnetic fields, Physical Review Applied **24**, 064049 (2025).